PCCP

Dynamic Article Links

Cite this: *Phys. Chem. Chem. Phys.*, 2011, **13**, 1466–1478

www.rsc.org/pccp

PAPER

Selective transport of amino acids into the gas phase: driving forces for amino acid solubilization in gas-phase reverse micelles

Yigang Fang, Andrew Bennett and Jianbo Liu*

Received 8th June 2010, Accepted 16th November 2010
DOI: 10.1039/c0cp00823k

We report a study on encapsulation of various amino acids into gas-phase sodium bis(2-ethylhexyl) sulfosuccinate (NaAOT) reverse micelles, using electrospray ionization guided-ion-beam tandem mass spectrometry. Collision-induced dissociation of mass-selected reverse micellar ions with Xe was performed to probe structures of gas-phase micellar assemblies, identify solute–surfactant interactions, and determine preferential incorporation sites of amino acids. Integration into gas-phase reverse micelles depends upon amino acid hydrophobicity and charge state. For examples, glycine and protonated amino acids (such as protonated tryptophan) are encapsulated within the micellar core *via* electrostatic interactions; while neutral tryptophan is adsorbed in the surfactant layer. As verified using model polar hydrophobic compounds, the hydrophobic effect and solute-interface hydrogen-bonding do not provide sufficient driving force needed for interfacial solubilization of neutral tryptophan. Neutral tryptophan, with a zwitterionic structure, is intercalated at the micellar interface between surfactant molecules through complementary effects of electrostatic interactions between tryptophan backbone and AOT polar heads, and hydrophobic interactions between tryptophan side chain and AOT alkyl tails. Protonation of tryptophan could significantly improve its incorporation capacity into gas-phase reverse micelles, and displace its incorporation site from the micellar interfacial zone to the core; protonation of glycine, on the other hand, has little effect on its encapsulation capacity. Another interesting observation is that amino acids of different isoelectric points could be selectively encapsulated into, and transported by, reverse micelles from solution to the gas phase, based upon their competition for protonation and subsequent encapsulation within the micellar core.

I. Introduction

With surfactant hydrophilic polar heads oriented around an approximately spherical, nanoscopic internal core and hydrophobic alkyl chains forming the outer surface, reverse micelles represent polar microenvironments and are extensively used for solubilization, separation, catalysis, nanoparticle synthesis, and as membrane-mimetic systems.[1–3] Although traditionally generated and utilized in apolar solvents or supercritical fluids,[3–5] reverse micelles have also been detected in marine aerosols[6–8] and upper tropospheric aerosols.[9] Aerosols of gas-phase reverse micelles are initially formed by surfactants of biological origin *via* wave action and mechanical ejection from the ocean surface, *i.e.*, ocean surfaces are covered by biologically-derived phospholipids and fatty acids that may incorporate onto the surface of marine aerosol particle, and form a spherical monolayer enclosing an aqueous interior.[10] Reverse micellar aerosols take up organic molecules from the ocean water, are transported by the general circulation of the atmosphere and exposed to various temperatures, pressures, radiation, and chemical attacks.[6–9,11,12] During these processes, reverse micelles act as vehicles for atmospheric transport[12] and may have provided an environment conducive to prebiotic chemical reactions.[13,14]

Amino acids (free and combined forms) are ubiquitous in marine and tropospheric aerosols,[15–18] and are believed to be intimately involved in reactions present in prebiotic milieux.[13] Therefore, encapsulation and transport of amino acids by gas-phase reverse micelles should be important for experimental investigation from the perspective of atmospheric chemistry and the evolution of amino acids to biopolymers. In addition, encapsulation of amino acids and other biomolecules into gas-phase reverse micelles allows new inroads for biophysical and bioanalytical research since gas-phase reverse micelles may be able to protect non-covalent interactions between encapsulated biomolecular subunits,[19] allowing analysis of their properties under constrained environments in a vacuum, like that used in mass spectrometry[19] and single particle imaging.[20] We recently reported formation of multiply charged sodium bis(2-ethylhexyl)

Department of Chemistry and Biochemistry, Queens College and the Graduate Center of the City University of New York, 65-30 Kissena Blvd., Flushing, New York 11367, USA. E-mail: jianbo.liu@qc.cuny.edu

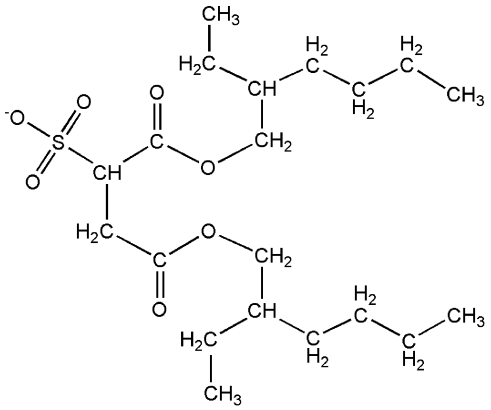

Fig. 1 Skeletal formula of bis(2-ethylhexyl) sulfosuccinate anion (AOT).

sulfosuccinate (NaAOT, structure shown in Fig. 1) reverse micelles in the gas phase using electrospray ionization (ESI)[21,22] guided-ion-beam methods, and characterized their structures using collision-induced dissociation (CID).[23] We found that, contrary to the general view that reverse micelles require water to "glue" the assembly,[24–27] no water molecules were present within gas-phase NaAOT reverse micelles. In addition, we found that gas-phase NaAOT reverse micelles are able to accommodate glycine molecules. Glycine was chosen for the encapsulation experiment because it is the most abundant amino acid molecule in atmospheric aerosols.[16,17] Analysis of CID fragment ions and CID cross sections of glycine-containing reverse micellar ions revealed their true reverse micelle-like structures with guest glycine molecules encapsulated within the micellar core. However, some interesting questions remained, particularly regarding the interactions of encapsulated amino acids with surfactants.

A great deal of work has been reported on determining driving forces for the uptake of amino acids into NaAOT and water reverse micelles in apolar media.[5,28–37] In sum, hydrophilic amino acids, both zwitterionic[38] and charged forms, are predominately hosted inside the micellar water pools,[33] and favorable electrostatic interactions would lead to increased solubilization of hydrophilic amino acids as verified by pH variation experiments.[34–36] Hydrophobic amino acids,[39–41] on the other hand, are mainly incorporated in the interfacial surfactant layer *via* favorable hydrophobic interactions, and electrostatic interactions may alter partitioning of hydrophobic amino acids between interfacial zones and water pools. Much less is known about encapsulation of amino acids by gas-phase reverse micelles, however. Gas-phase reverse micelles eliminate external apolar solvents as well as internal water molecules, forming more compact structures with surfactant tails collapsing on the outer surface.[42,43] This leads to an interesting question: what forces drive the solubilization of amino acids into gas-phase reverse micelles? Our work aims at exploring the solubilization driving forces and site localizations of amino acids in gas-phase reverse micelles, as well as how they could be tuned. First, using ESI mass spectrometry, we compared encapsulation of various amino acids (and their model compounds) in gas-phase NaAOT reverse micelles. Second, from collision-induced dissociation of amino acid-encapsulating reverse micellar ions, we determined the site locations of amino acids of different hydrophobicities and charge states within gas-phase reverse micelles. Finally, different interactions between amino acids and reverse micelles were explored for selective encapsulation of amino acids by gas-phase reverse micelles.

II. Experimental details

NaAOT (sodium bis(2-ethylhexyl) sulfosuccinate, $C_{20}H_{37}NaO_7S$, molecular weight 444, >99.0%) was supplied by Fluka and stored over P_2O_5 in a desiccator. Glycine (≥ 99%), L-arginine (>98.5%), L-aspartic acid (>99%), L-tryptophan (99%), L-tyrosine (≥ 99%), β-naphthol (99%), phloretic acid (98%) and anhydrous hexane (95%) were purchased from Sigma Aldrich, phenol (99%) was obtained from Alfa Aesar, and sodium hydroxide (>97%) was obtained from Fisher Chemicals. Table 1 lists the structures of some amino acids under study, and the values of their ionization constants (pK_a) and isoelectric points (pI) in aqueous solutions. All chemicals were used without further purification. Methanol and water used in experiments were HPLC grade (Fisher Chemicals).

The guided-ion-beam tandem mass spectrometer used in this study has been described previously,[23,44] along with the operation, calibration and data analysis procedures. Only a brief description is given here, emphasizing the unique features of this experiment. The apparatus consists of an ion source, radio frequency (rf) hexapole ion guide,[45] quadrupole mass filter, rf octopole ion guide surrounded by a scattering cell, second quadrupole mass filter and a detector. Both quadrupole mass filters use Extrel 9.5 mm diameter tri-filter rods operating at 880 kHz (Extrel model 150 QC) to cover a mass/charge

Table 1 Molecular structures, ionization constants and isoelectric points of various amino acids[a]

Amino acid	Aspartic acid (D^b)	Tryptophan (W^b)	Arginine (R^b)
Structure	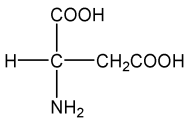	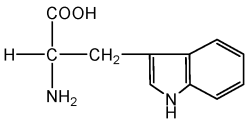	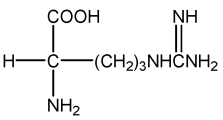
pK_a of α-COOH	1.9	2.8	2.2
pK_a of α-NH_3^+	9.6	9.4	9.0
pK_a of side chain	3.7	—	12.5
pI	2.8	5.9	10.8

[a] Values of pK_a and pI are from ref. 38 and were determined in aqueous solutions. [b] One-letter code for amino acid.

range from 1 to 4000. For conventional mass spectral measurements, the first quadrupole mass filter was operated in the rf-only mode as an ion guide, and mass scans were performed by the second quadrupole mass filter. The mass resolution ($R = m/\Delta m$) of the instrument was adjusted to 200 (or higher) for most of the measurements. The resolution was sufficient to resolve the charge state and stoichiometry of micellar ions without significantly decreasing the ion intensities.

It was recently demonstrated that reverse micelles can be produced in the vacuum of a mass spectrometer,[23,46–49] using ESI methods. In our previous report,[23] multiply charged gas-phase NaAOT reverse micelles were generated using ESI of NaAOT/water–hexane reverse micellar solutions with controlled water loading ($\omega_0 = [H_2O]/[NaAOT] = 5$–20). To prepare amino acid-containing reverse micelles, amino acids were first dissolved in aqueous solution, and then injected into reverse micelles in hexane. The advantage of using a micellar solution for ESI is that pre-formed reverse micelles, when transferred from solution to the gas phase, may be able to preserve their structures (at least to some extent) and thus help form larger gas-phase micellar aggregates. This hypothesis was confirmed by our observation that gas-phase NaAOT reverse micelles generated from ESI of reverse micellar solutions have greater aggregation numbers and charges compared to those from ESI of NaAOT monomer solutions in dry hexane or methanol–water.[23] However, amino acids could not dissolve in hexane. Consequently, this preparation method could only incorporate hydrophilic amino acids, with substantial aqueous solubilities (*e.g.* glycine and proline), into the water pools of reverse micelles in hexane. A different approach was used in our current experiments. ESI solutions were prepared in methanol–water (1 : 1 volume ratio) containing 1.0×10^{-3} M NaAOT (below the CMC in water, 2.0×10^{-3} M,[50] so that reverse micelles were not formed) and 0.2×10^{-3} M amino acid (*e.g.* tryptophan). The solution was sonicated for 10 min prior to ESI. The pH of the solution was measured using a Thermo Scientific Orion 3-Star pH meter. As demonstrated below, NaAOT and amino acids were able to form amino acid-encapsulating reverse micelles *via* self-assembling in the gas phase between electrospray and exposure to the high vacuum of the mass spectrometer.[23,47] This fresh approach overcomes amino acid aqueous solubility limitations, allowing various amino acids (both hydrophilic and hydrophobic) to be transported by electrospray and incorporated into gas-phase reverse micelles.

The NaAOT/amino acid solution was sprayed into the ambient atmosphere through an electrospray needle using a syringe pump (KD Scientific model 100), at a constant flow rate of 0.04 ml h^{-1}. The electrospray needle was prepared from 35-gauge hypodermic stainless steel tubing (0.13 mm o.d. × 0.06 mm i.d., Small Parts Inc.), and biased at 3000 V relative to ground. Positively charged droplets formed from the electrospray needle were fed into a heated desolvation capillary. Initial radii of spray droplets are estimated to be ~0.9 μm.[51–53] Assuming solvent evaporates uniformly from the droplet surface, the time for hexane evaporation is estimated to be less than 1 ms.[54] The distance between the electrospray needle tip and the sampling orifice of the capillary was ~1 cm. The capillary was biased at 70 V relative to ground and heated to 150 °C. Charged liquid droplets underwent desolvation as they passed through the heated capillary, converting to charged gas-phase reverse micelles. A skimmer with an orifice of 1.5 mm (Beam Dynamics, Inc.) was located 2.5 mm from the capillary end, separating the ion source chamber and the hexapole ion guide. The skimmer was biased at 10 V relative to ground, and the electrical field between the capillary and the skimmer helped eliminate remaining solvent molecules by collision-induced desolvation.[55] Reverse micellar ions that emerged from the skimmer were passed into a rf hexapole ion guide at a pressure of 10–15 mTorr, leading to collisional focusing.[56–58] Ions subsequently passed into a set of entrance focusing lenses followed by the first quadrupole mass filter for mass selection. Mass-selected reverse micellar ions were then injected into a rf octopole ion guide which trapped ions in the radial direction. The octopole ion guide operated at 2.6 MHz with a peak-to-peak amplitude of 700 V. DC bias voltage was applied to the ion guide with its amplitude varying from −500 to +500 V. The dc bias voltage was used in the retarding potential analysis (RPA)[59] to determine the initial kinetic energy of selected reverse micellar ions, *i.e.*, intensities of ions were measured while sweeping the octopole bias. The dc bias voltage also allowed control of the kinetic energy of reverse micellar ions in the laboratory frame. Reverse micellar ion kinetic energies in the lab frame (E_{lab}) are converted to collision energies in the center-of-mass frame (E_{col}) using $E_{col} = E_{lab} \times m_{neutral}/(M_{ion} + m_{neutral})$, where $m_{neutral}$ and M_{ion} are masses of neutral collision gas and reverse micellar ions, respectively. The octopole passed through a scattering cell containing the collision gas Xe (Spectral Gases, 99.995%). The scattering cell pressure was measured by a capacitance manometer (MKS Baratron 690 head and 670 signal conditioner). CID product ion mass spectra of mass-selected NaAOT reverse micellar ions were measured at $E_{col} = 1.0$ eV for doubly charged ions and $E_{col} = 1.5$ eV for triply charged ions. Precursor reverse micellar ions and their fragment ions were collected by the octopole ion guide, and directed to the second mass spectrometer for mass analysis. Ion signals were counted using a pulse-counting electron multiplier (DeTech model 411). CID cross sections at each different E_{col} were calculated based on the loss of precursor ions, the target gas pressure, and the calibrated effective length of the scattering cell.[23,44] All measurements were repeated at least three times.

III. Results and discussion

A Solubilization of neutral and protonated tryptophan in gas-phase reverse micelles

1 Dependence of amino acid hydrophobicity and charge state on incorporation capacity into gas-phase reverse micelles. Tryptophan has the most hydrophobic side chain (*i.e.* indole ring) of all amino acids,[39] but becomes hydrophilic upon protonation. Choosing neutral and protonated tryptophan as guest molecules allows us to examine both hydrophobic effect and electrostatic effect in gas-phase reverse micelles. Fig. 2a shows a mass spectrum obtained from ESI of NaAOT (1.0×10^{-3} M) and tryptophan (0.2×10^{-3} M) in methanol–water. For the sake

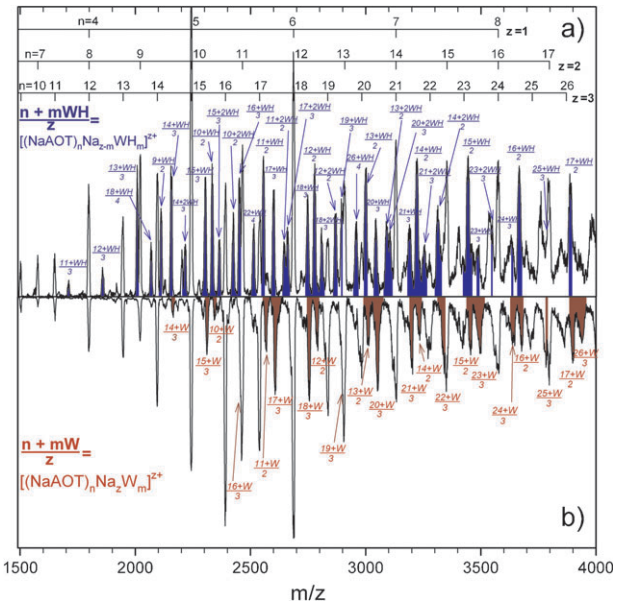

Fig. 2 ESI mass spectra of NaAOT reverse micellar ions containing (a) protonated tryptophan (*WH*) and (b) neutral tryptophan (*W*).

of clarity, the mass/charge range below 1500 is not shown, but no encapsulation of tryptophan was observed at that range. It was found that, within the instrument detection range, the dominant peaks belong to empty reverse micelles with the compositions of $[(\mathrm{NaAOT})_n\mathrm{Na}_z]^{z+}$. Assignments of mass peaks of empty reverse micelles are based on the micellar aggregation numbers (n) and charges (z), and the labels for the same charge states are grouped together. For convenience, in the following discussion the empty reverse micelles are indicated as n/z. The pH of the ESI solution was measured at 6.1, which is close to the tryptophan isoelectric point (pI) of 5.9 reported in an aqueous solution. However, it can be expected that pH may increase dramatically in the electrospray droplets due to the nature of positive mode ESI processes. In addition, there may exist difficulties in ionizing the –COOH group of tryptophan, due to its proximity to AOT anionic head groups.[60] As a result, protonated tryptophan (henceforth designated as *WH*) was incorporated into reverse micelles and detected in the mass spectrum with the compositions of $[(\mathrm{NaAOT})_n\mathrm{Na}_{z-m}WH_m]^{z+}$. These are indicated in shaded areas and labeled $(n + mWH)/z$. Solubilization of protonated tryptophan can be viewed as an ion-exchange process between positively charged *WH* and Na^+ ions.[34,36] To investigate the hydrophobic effect of the tryptophan indole group, we adjusted the ESI solution pH to 7.9 by adding NaOH to a concentration of 0.2×10^{-3} M in methanol–water. With these conditions, only neutral tryptophan (hereafter designated as *W*) was carried into gas-phase reverse micelles by ESI, with the compositions of $[(\mathrm{NaAOT})_n\mathrm{Na}_z\mathrm{W}_m]^{z+}$. *W*-encapsulating reverse micelles are indicated in shaded areas in Fig. 2b, and labeled $(n + mW)/z$.

Fig. 2a and b show a strong correlation between size and incorporation capability of gas-phase reverse micelles. For doubly charged reverse micelles, incorporation of protonated tryptophan starts from aggregation number $n = 9$, and micelles of $n \geq 10$ can entrap two protonated tryptophan molecules. Triply charged reverse micelles start incorporating tryptophan at $n = 11$, and micelles of $n \geq 14$ can entrap two protonated tryptophan molecules. Assuming a spherical reverse micelle-like geometry for NaAOT aggregates, its core diameter D is roughly equal to $\sqrt{n \times A_{\mathrm{head}}/\pi}$ where A_{head} is the area occupied by each AOT polar head at the interface (0.52 nm^2).[1,5,61] D is calculated to be 1.2, 1.3, 1.4, and 1.6 nm for $n = 9$, 10, 11 and 14, respectively. The orientation-averaged size of a protonated tryptophan molecule is 0.5–0.6 nm. Taking into account the volume occupied by counter ions, Na^+, the number of encapsulated protonated tryptophan molecules roughly matches the reverse micellar core size. For comparison, incorporation of neutral tryptophan starts from $n = 10$ for doubly charged micelles, and $n = 14$ for triply charged micelles, respectively. Incorporation of more than one neutral tryptophan molecule in single micelles was not observed in Fig. 2b. For both protonated and neutral tryptophan, the starting aggregation numbers for incorporation remained constant when the initial tryptophan-loading ratio to NaAOT, [tryptophan]/[NaAOT], varied from 10 : 1 to 10 : 3 in ESI solutions. These observations deviate from expectations if random associations are assumed between amino acids and surfactants. Similar results were obtained using protonated and neutral tyrosine as guest molecules for gas-phase NaAOT reverse micelles (mass spectra not shown), where the incorporation of protonated and neutral tyrosine both starts from $n = 8$ for doubly charged reverse micelles, and $n = 11$ for triply charged reverse micelles, respectively.

The fact that neutral hydrophobic amino acids (tryptophan and tyrosine) can be incorporated into gas-phase reverse micelles does not necessarily confirm that the hydrophobic effect is the major driving force for solubilization, since neutral amino acids most likely exist in zwitterionic forms and maintain some solute-surfactant electrostatic interactions. With this in mind, control experiments were performed using methanol–water solutions of NaAOT with various probe molecules, including phenol, β-naphthol and phloretic acid. Phenol and β-naphthol were used as probe molecules because they resemble the uncharged polar side chains of tryptophan and tyrosine, and can reside at the interface of NaAOT reverse micelles in apolar solvents (*e.g.* *n*-heptane and isooctane) as co-surfactants, with their hydroxyl groups hydrogen-bonded to AOT polar heads and aromatic rings penetrating between AOT hydrocarbon tails.[1,60,62,63] Phloretic acid was chosen since it is actually a tyrosine analogue with only the amino group is absent from the tyrosine structure. We measured the ESI mass spectra of the solutions containing NaAOT and each of the three probe molecules, respectively, following the same procedures used for NaAOT/amino acids. Their solution pH was not adjusted intentionally, *i.e.*, pH 6.5 for NaAOT (1.0×10^{-3} M)/phenol (0.2×10^{-3} M) and NaAOT(1.0×10^{-3} M)/β-naphthol (0.2×10^{-3} M) in methanol–water, and pH 4.8 for NaAOT (1.0×10^{-3} M)/phloretic acid (0.2×10^{-3} M) in methanol–water. Surprisingly, none of the three probe molecules were observed within gas-phase NaAOT reverse micelles. It may be argued that phenol and β-naphthol could not effectively incorporate onto the micellar interface during self-assembling of NaAOT reverse micelles in the gas phase. For this reason, we also measured ESI mass spectra of NaAOT

(5.0×10^{-3} M)/water (5.0×10^{-2} M)/hexane reverse micellar solutions containing 1×10^{-3} M phenol and β-naphthol, respectively. The NaAOT concentration used is above its CMC in hexane[50] to ensure the formation of NaAOT and water reverse micelles in hexane as well as adsorption of phenol or β-naphthol at the water pool interface. Again, neither phenol nor β-naphthol was detected in the ESI mass spectra. Obviously, the hydrophobic effect and hydrogen bonding are not strong enough to incorporate phenol and β-naphthol onto the surface of gas-phase reverse micelles. From the fact that phloretic acid could not be incorporated, we infer that the carboxylic acid group alone (without the amino group in the molecule) does not help achieve a great enough driving force for incorporation of the molecule into gas-phase reverse micelles, either. Consequently, neutral *zwitterionic* tryptophan (and tyrosine) must have the charged $-NH_3^+$ group strongly interact with AOT sulfonic group. It is the combination of hydrophobic and electrostatic interactions that allows incorporation of neutral tryptophan (and tyrosine) into gas-phase reverse micelles.

It would be interesting to compare incorporation of protonated and neutral amino acids qualitatively. For this purpose, we calculated relative incorporation efficiencies defined as

$$E_{WH} = \frac{I([(\mathrm{NaAOT})_n\mathrm{Na}_{z-1}WH]^{z+})}{I([\mathrm{NaAOT})_n\mathrm{Na}_z]^{z+})} \quad (1)$$

and

$$E_{W} = \frac{I([(\mathrm{NaAOT})_n\mathrm{Na}_{z}W]^{z+})}{I([\mathrm{NaAOT})_n\mathrm{Na}_z]^{z+})} \quad (2)$$

where $I([(NaAOT)_nNa_{z-1}WH]^{z+})$, $I([(NaAOT)_nNa_zW]^{z+})$ and $I([(NaAOT)_nNa_z]^{z+})$ represent measured ion intensities of *WH*-, *W*-encapsulating, and empty host reverse micellar ions, respectively. To avoid complication of mass coincidence of selected host micellar ions with other charge states, we chose $[(NaAOT)_nNa_z]^{z+}$ of 13/2, 15/2, 17/2, 14/3, 16/3, 17/3 and 20/3 as host micellar ions for analysis. NaAOT reverse micellar ions can each encapsulate more than one *WH* molecule; however, the contributions of multiple encapsulations of *WH* were not included when calculating incorporation efficiencies E_{WH}. This omission was deliberate, since reverse micellar ions can only take one *W* molecule each. For direct comparison of incorporation efficiencies for *WH* and *W*, we chose to focus on encapsulation of single molecules in both cases. The calculation results are listed in Table 2, and were averaged over three sets of mass spectra. For comparison, we have included in Table 2 the incorporation efficiencies E_{GH} and E_G (*i.e.*, efficiencies of incorporating one protonated glycine and one neutral glycine in NaAOT reverse micellar ions, respectively), calculated from our previous experimental data.[23] These calculations give very rough estimates, but are sufficient to reveal general trends. Clearly, protonation dramatically increases the incorporation efficiencies of tryptophan for all reverse micelles, but has little effect on incorporation efficiencies of glycine.

The differences between E_{WH} and E_W, and between E_{GH} and E_G, arise from the extra electrostatic interactions between protonated amino acids and anionic AOT polar heads. It was found that, on average, this extra electrostatic effect improves incorporation efficiencies of tryptophan by a factor of 2–3. Note that the enhancement ratio of E_{WH}/E_W decreases rapidly with increasing micellar size, and approaches a minimum for reverse micelles of 20/3. This is simply due to the fact that large micelles can hold more *WH* molecules. For glycine, there is no hydrophobic contribution and an attractive electrostatic potential is needed for solubilization of this amino acid in reverse micelles. Therefore, we would expect a large increase in incorporation when glycine becomes protonated. However, there is no dramatic difference between E_{GH} and E_G. Only a slight enhancement of E_{GH}/E_G was observed upon protonation of glycine (except for micelles of 15/2 and 17/2, where protonation causes a minor decrease in the uptake of single amino acids, presumably because the fraction of reverse micelles containing more than one glycine molecule increases upon protonation of glycine). We tentatively attribute the observed small differences between E_G and E_{GH} to the fact that neutral zwitterionic glycine structure can interact with sodium ions and AOT polar heads inside the micellar cavity and becomes stabilized by these electrostatic interactions. We note that in the gas phase the glycine–Na^+ binding energy is 1.7 eV,[64,65] and proton affinity of glycine is 9.2 eV.[66] However, the gas-phase affinity values seem have very little connection with the expected behavior in condensed phase or in gas-phase reverse micelles.

2 Solubilization sites of hydrophilic and hydrophobic amino acids. Fig. 3 shows the CID product ion mass spectra of *WH*-encapsulating reverse micellar ions, measured at $E_{col} = 1.0$ eV for doubly charged precursor ions and 1.5 eV for triply charged precursor ions. To map out all dissociation product ions within the instrumental mass/charge detection limit, CID mass spectra were obtained at a relatively high Xe pressure (0.15 mTorr) in the scattering cell. Because of multiple collisions between precursor ions and Xe at this gas pressure, and because primary fragment ions may continue to undergo collisions that cause them to fragment, the relative intensities of product ions in CID mass spectra do not reflect CID branching ratios. However, all product ions were observed at a Xe pressure of 0.01–0.013 mTorr, where the probability of multiple collisions is $<4\%$. CID of multiply charged reverse micellar ions results in numerous dissociation channels and product ions of varying mass and charge, and some product ions may possess mass/charge that is beyond the instrument detection limit. In addition, because of mass coincidence among different charged states, some ion peaks may actually be attributed to more than one product ion mass. For example, mass/charge of 3131 may represent micelles of three overlapping charge states 7/1, 14/2, and 21/3. In Fig. 3, alternative assignments for some product ions are indicated in parentheses.

Table 3 summarizes dissociation channels for selected *WH*-encapsulating reverse micellar ions. For most dissociation channels, both complementary product ions produced from a dissociation leading to two charged products were observed in mass spectra. For comparison, we have also included in Table 3 the CID results of corresponding neutral Gly-encapsulating NaAOT reverse micellar ions as well as empty reverse micellar ions obtained from a previous study.[23] Because glycine and protonated tryptophan are both hydrophilic, similarities would be expected in dissociation of reverse micelles containing these two amino acids.

Table 2 Incorporation efficiencies of protonated (*WH*) and neutral (*W*) tryptophan, and protonated (*GH*) and neutral (*G*) glycine in gas-phase NaAOT reverse micellar ions

Host reverse micellar ions[a]	E_{WH}	E_W	E_{WH}/E_W	E_{GH}	E_G	E_{GH}/E_G
$\frac{13}{2}$	1.11	0.34	3.3	0.82	0.60	1.4
$\frac{15}{2}$	1.03	0.62	1.7	0.78	0.90	0.9
$\frac{17}{2}$	1.09	0.70	1.6	1.30	1.50	0.9
$\frac{14}{3}$	1.06	0.20	5.3	0.65	0.50	1.3
$\frac{16}{3}$	1.04	0.40	2.6	0.83	0.71	1.2
$\frac{17}{3}$	1.25	0.67	1.9	1.00	0.94	1.1
$\frac{20}{3}$	1.42	1.10	1.3	1.25	1.20	1.0

[a] Host reverse micellar ions are indicated as $\frac{n}{z}$, where n is the aggregation number, and z is the total charge.

As shown in Fig. 3 and Table 3, dissociation of reverse micellar ions strongly depends on their charge state and encapsulation. CID of doubly charged empty NaAOT reverse micellar ions exclusively produces singly charged fragment ions, while CID of triply charged empty NaAOT reverse micellar ions results in singly, doubly and triply charged ions.[23] Occupied reverse micellar ions have distinct dissociation channels from empty ones, producing large product ions, some of which still encapsulate amino acids. This suggests that amino acid encapsulation improves the overall stability of reverse micellar structures. It is worthwhile to mention that all listed pairs of *WH*- and Gly-encapsulating reverse micellar ions, (15 + *WH*)/2 and (15 + *G*)/2, (17 + *WH*)/2 and (17 + *G*)/2, (17 + *WH*)/3 and (17 + *G*)/3, and (20 + *WH*)/3 and (20 + *G*)/3, exhibit similar dissociation patterns. In Fig. 2a (*i.e.* a mass spectrum of *WH*-encapsulating micellar ions) we observed a strong correlation between the encapsulation capability and the size of micellar ions. Similar behavior was observed in CID mass spectra of *WH*-encapsulating reverse micelles. The smallest stripped micellar ions still capable of hosting protonated tryptophan are 11/2.

In a previous study,[23] we measured CID cross sections for mass-selected empty and Gly-encapsulating precursor reverse micellar ions, and found that CID cross sections are approaching the hard-sphere collision limits at high collision energies (if we assume spherical geometries for reverse micellar ions). The cross sections provided a measure of the lowest limit of the average micelle size. We also attempted to measure CID cross sections at various collision energies for this system. Unfortunately, the low intensities of selected *WH*-encapsulating precursor ions made it exceedingly difficult to achieve good signal-to-noise ratios for measurements at a Xe pressure of 0.01 mTorr (which was required to ensure a single-collision condition between micellar ions and Xe). Note that, while we were not able to measure the CID cross section as a function of E_{col} accurately, CID cross sections generally increase with increasing E_{col} and the maximum CID cross sections of *WH*-encapsulating reverse micellar ions seem close to those of corresponding Gly-encapsulating reverse micellar ions. The resemblance between CID products and cross sections of *WH*- and Gly-encapsulating reverse micellar ions are so striking that they make clear the conclusion that protonated tryptophan is encapsulated inside the micellar core and attracted to AOT head groups near the interface. This is similar to the site location of protonated tryptophan in NaAOT/water reverse micelles immersed in apolar media such as n-heptane and dichloroethane,[33,37] and is consistent with the molecular dynamics simulated solute location of positively charged chromophore in NaAOT reverse micelles.[67]

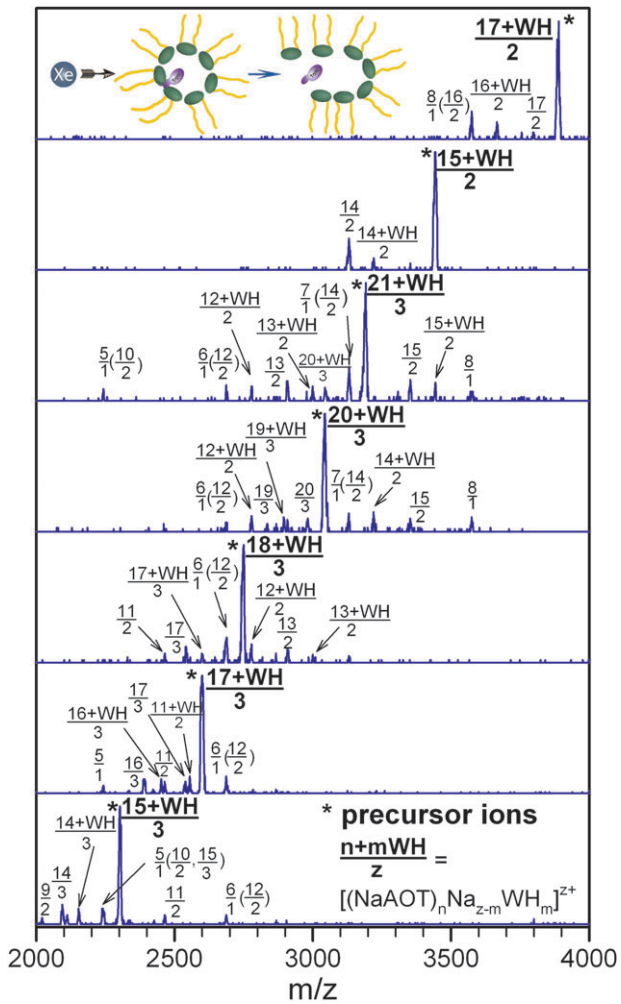

Fig. 3 CID mass spectra of mass-selected micellar ions containing protonated tryptophan (*WH*). Spectra were measured at E_{col} = 1.0 eV for doubly charged precursor ions and E_{col} = 1.5 eV for triply charged precursor ions, with 0.15 mTorr Xe in the scattering cell. Asterisks indicate precursor ions, and labels in parentheses are alternative assignments for product ions. Inserted cartoon illustrates encapsulation of *WH* within the gas-phase reverse micellar core.

CID of mass-selected reverse micellar ions containing neutral tryptophan, *W*, as depicted in Fig. 4, reveals different

Table 3 CID products of empty and amino acid-encapsulating NaAOT micellar ions

WH-encapsulating micellar ions[a]	Dissociation channels	Gly-encapsulating micellar ions[b]	Dissociation channels	Empty micellar ions[b]	Dissociation channels
$\frac{15+WH}{2}$	$\frac{14+WH}{2}+1$	$\frac{15+G}{2}$	$\frac{13}{2}+2+G$	$\frac{15}{2}$	$\frac{9^c}{1}+\frac{6}{1}$
	$\frac{14}{2}+1+WH$		$\frac{14}{2}+1+G$		$\frac{8}{1}+\frac{7}{1}$
$\frac{17+WH}{2}$	$\frac{17}{2}+WH$	$\frac{17+G}{2}$	$\frac{16+G}{2}+1$	$\frac{17}{2}$	$\frac{11^c}{1}+\frac{6}{1}$
	$\frac{16+WH}{2}+1$		$\frac{9^c}{1}+\frac{8}{1}+G$		$\frac{10^c}{1}+\frac{7}{1}$
	$\frac{16}{2}+1+WH$				$\frac{9^c}{1}+\frac{8}{1}$
	$\frac{9^c}{1}+\frac{8}{1}+WH$				
$\frac{15+WH}{3}$	$\frac{14+WH}{3}+1$				
	$\frac{14}{3}+1+WH$				
	$\frac{10}{2}+\frac{5}{1}+WH$				
	$\frac{9}{2}+\frac{6}{1}+WH$				
	$\frac{11}{2}+\frac{4}{1}+WH$				
$\frac{17+WH}{3}$	$\frac{17}{3}+WH$	$\frac{17+G}{3}$	$\frac{16+G}{3}+1$	$\frac{17}{3}$	$\frac{16}{3}+1$
	$\frac{16+WH}{3}+1$		$\frac{16}{3}+1+G$		$\frac{12}{2}+\frac{5}{1}$
	$\frac{16}{3}+1+WH$		$\frac{12}{2}+\frac{5}{1}+G$		$\frac{11}{2}+\frac{6}{1}$
	$\frac{12}{2}+\frac{5}{1}+WH$		$\frac{11}{2}+\frac{6}{1}+G$		$\frac{9}{2}+\frac{8}{1}$
	$\frac{11+WH}{2}+\frac{6}{1}$				

Table 3 (*continued*)

WH-encapsulating micellar ions[a]	Dissociation channels	Gly-encapsulating micellar ions[b]	Dissociation channels	Empty micellar ions[b]	Dissociation channels
	$\frac{11}{2}+\frac{6}{1}+WH$				
$\frac{18+WH}{3}$	$\frac{17+WH}{3}+1$				
	$\frac{17}{3}+1+WH$				
	$\frac{13+WH}{2}+\frac{5}{1}$				
	$\frac{13}{2}+\frac{5}{1}+WH$				
	$\frac{12+WH}{2}+\frac{6}{1}$				
	$\frac{12}{2}+\frac{6}{1}+WH$				
	$\frac{11}{2}+\frac{7}{1}+WH$				
$\frac{20+WH}{3}$	$\frac{20}{3}+WH$	$\frac{20+G}{3}$	$\frac{19+G}{3}+1$	$\frac{20}{3}$	$\frac{14}{2}+\frac{6}{1}$
	$\frac{19+WH}{3}+1$		$\frac{19}{3}+1+WH$		$\frac{13}{2}+\frac{7}{1}$
	$\frac{19}{3}+1+WH$		$\frac{13+G}{2}+\frac{7}{1}$		$\frac{12}{2}+\frac{8}{1}$
	$\frac{14+WH}{2}+\frac{6}{1}$		$\frac{13}{2}+\frac{7}{1}+G$		$\frac{11}{3}+\frac{9^c}{1}$
	$\frac{14}{2}+\frac{6}{1}+WH$				$\frac{10}{2}+\frac{10^c}{1}$
	$\frac{12+WH}{2}+\frac{8}{1}$				
	$\frac{12}{2}+\frac{8}{1}+WH$				
$\frac{21+WH}{3}$	$\frac{20+WH}{3}+1$				

Table 3 (*continued*)

WH-encapsulating micellar ions[a]	Dissociation channels	Gly-encapsulating micellar ions[b]	Dissociation channels	Empty micellar ions[b]	Dissociation channels
	$\frac{16}{2}+\frac{5}{1}+WH$				
	$\frac{15+WH}{2}+\frac{6}{1}$				
	$\frac{15}{2}+\frac{6}{1}+WH$				
	$\frac{14}{2}+\frac{7}{1}+WH$				
	$\frac{13+WH}{2}+\frac{8}{1}$				
	$\frac{13}{2}+\frac{8}{1}+WH$				
	$\frac{12+WH}{2}+\frac{9^{c}}{1}$				
	$\frac{12}{2}+\frac{9^{c}}{1}+WH$				

[a] Precursor and product ions are indicated as $\frac{n+mWH}{z}$ for those containing protonated tryptophan (*WH*), $\frac{n+mG}{z}$ for those containing glycine (G), and $\frac{n}{z}$ for empty micelles, where n is the aggregation number, z is the total charge, and m is the number of encapsulated amino acids. [b] From ref. 23. [c] Beyond the mass/charge detection limit of the mass spectrometer.

dissociation patterns than those containing *WH* and glycine. Dissociation of *W*-encapsulating reverse micellar ions corresponds to stripping *W* (and only *W* moiety) off reverse micelles. Such CID results provide direct evidence of the location of the incorporation site of neutral tryptophan, *i.e.*, neutral tryptophan must adsorb to the micellar surface, due to its hydrophobic nature. This scenario raises two possibilities. Neutral tryptophan could either penetrate into the surfactant polar head layer as a co-surfactant,[31] or randomly tether to and/or embed in AOT hydrophobic tails following the principle of "like dissolves like". The second possibility may be discounted for several reasons. First, if we assume random associations between tryptophan and AOT, we would have observed associations between tryptophan and small NaAOT aggregates. In fact, NaAOT reverse micelles demonstrate strong size dependence for incorporation of neutral tryptophan. Incorporation of tryptophan starts from reverse micelles with aggregation number $\geq$ 10. Secondly, as described above, polar hydrophobic molecules such as phenol and β-naphthol could not be carried by gas-phase NaAOT reverse micelles at all, implying that the hydrophobic effect (of the tryptophan indole group) is unable to allow the micellar assembly of NaAOT and neutral tryptophan survive in the gas phase. Thirdly, the control experiment using the tyrosine model molecule, phloretic acid, confirmed that the carboxylic acid group, in the absence of an amino group, does not help satisfy the forces for incorporation of amino acid. All these facts lead to the conclusion that neutral tryptophan must have intercalated in the surfactant interfacial layer, acting as a co-surfactant based on a "surface-monolayer" model where the solute is adsorbed into the interface.[28–31] The driving forces for incorporation have contributions from the hydrophobic effect of the indole group with AOT branched alkyl tails; and more importantly, from the electrostatic interactions between the zwitterionic backbone $^{+}H_3N–C^{\alpha}–COO^{-}$ and the anionic AOT sulfonic polar head.[36] Repulsion between the zwitterion carboxylate group and the AOT anionic polar head may exist, but this can be compensated by the attraction between the carboxylate group and the Na^{+} ions which are located near the interface head region. The proposed incorporation mechanism for neutral tryptophan explains the reverse micelle size dependence of tryptophan incorporation capacity (see Fig. 2b). Small reverse micelles (*i.e.*, $n < 10$ for doubly charged micelles) have large curvatures, and consequently, cannot provide enough interfacial area (near head regions)

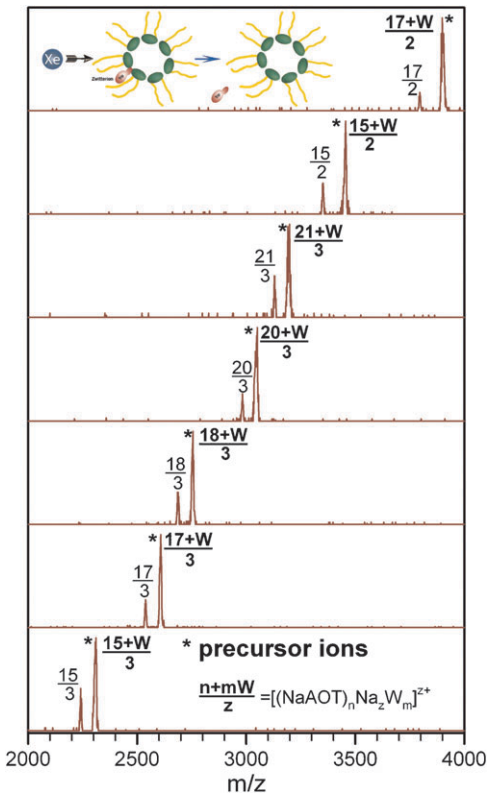

Fig. 4 CID mass spectra of mass-selected micellar ions containing neutral tryptophan (*W*). Spectra were measured at E_{col} = 1.0 eV for doubly charged precursor ions and E_{col} = 1.5 eV for triply charged precursor ions, with 0.15 mTorr Xe in the scattering cell. Asterisks indicate precursor ions. Inserted cartoon illustrates interfacial incorporation of *W* by gas-phase reverse micelles.

for incorporating guest tryptophan molecule. For triply charged micelles, the extra Na^+ makes the micelle more rigid and increases the curvature, so incorporation of neutral does not occur for $n < 14$.

Note that we cannot rule out the possibility that protonated tryptophan can partition between the reverse micellar inner core and the reverse micelle interfacial region. However, based on the comparison of CID mass spectra of *WH*- and *W*-encapsulating reverse micellar ions, protonated tryptophan predominantly partitions inside the core and its interfacial solubilization is negligible. Different site locations of protonated and neutral tryptophan also explain the observations in Fig. 2a and b that large reverse micelles have a higher capability of encapsulating *WH* inside the core than incorporating *W* outside—this is because the micellar core volume ($=(n \times A_{head})^{3/2}/6\pi^{1/2}$, where A_{head} is AOT polar head area as defined above) increases faster with the aggregation number *n* than the micellar interface area ($=n \times A_{head}$).

B Selective encapsulation of various amino acids by gas-phase reverse micelles

1 Aspartic acid *versus* tryptophan. The dependence of site localization of tryptophan on the pH of the ESI solution gives insight regarding the driving forces for gas-phase reverse micellar solubilization. It demonstrates that different experimental parameters may be used to control and manipulate the interactions between amino acid and NaAOT surfactants and therefore the incorporation site of the same amino acid within reverse micelles. It may also make selective incorporation of amino acids of different charge states possible. To investigate this possibility, we carried out experiments in the presence of two amino acids. We first chose aspartic acid and tryptophan, on the basis of their pI values. Aspartic acid is hydrophilic and has two carboxylic acid groups, with pK_{a1} 1.9, pK_{a2} 3.7, pK_{a3} 9.6, and pI 2.8 (lower than tryptophan pI 5.9 by 3.1 units). Fig. 5 shows the mass spectrum of an ESI solution containing NaAOT (1.0×10^{-3} M) and aspartic acid (0.1×10^{-3} M) in methanol–water with pH 4.6. As illustrated in Fig. 5, gas-phase reverse micelles are occupied by protonated aspartic acid (henceforth designated as *DH*). No neutral aspartic acid was observed; presumably because of the change of pH in the spraying droplets and of pK_a and pI of aspartic acid in reverse micelles.[36,60] However, all ion peaks associated with encapsulation of protonated aspartic acid disappeared after adding 0.1×10^{-3} M tryptophan to the ESI solution (pH changed to 5.1). Instead, a mass spectrum similar to Fig. 2a was obtained, where only protonated tryptophan was

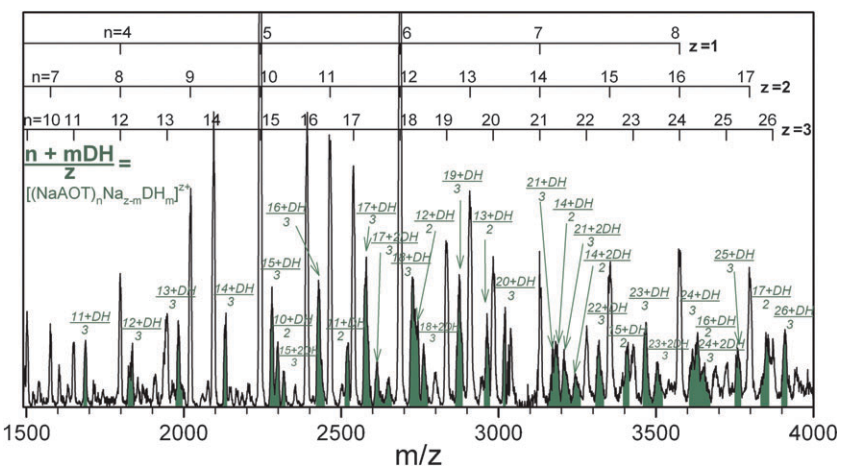

Fig. 5 ESI mass spectrum of gas-phase NaAOT reverse micellar ions containing protonated aspartic acid (*DH*).

encapsulated. In other words, gas-phase reverse micelles exclusively select protonated tryptophan.

2 Arginine *versus* tryptophan. We compared arginine and tryptophan in a similar fashion. Arginine has two amino groups, with pK_{a1} 2.2, pK_{a2} 9.0, pK_{a3} 12.5, and pI 10.8. As presented in Fig. 6, the mass spectrum of NaAOT (1.0×10^{-3} M), arginine (0.1×10^{-3} M) and tryptophan (0.1×10^{-3} M) in methanol–water (pH 7.5) only shows encapsulation of protonated arginine (designated as *RH*) in gas-phase reverse micelles. Observations of protonated tryptophan from a mixture of aspartic acid and tryptophan, and of protonated arginine from a mixture of arginine and tryptophan, as shown in Fig. 5 and 6, respectively, indicate that different amino acids are competing for protons in solutions and/or during ESI. The amino acid with a higher pI is more likely protonated, and the corresponding protonated species has a greater chance for encapsulation within the micellar core through electrostatic interactions with AOT anionic polar heads. As a result, the preference for encapsulation within the micellar core increases in ascending order of amino acid pI values, *i.e.*, aspartic acid (pI 2.8) < tryptophan (5.9) < arginine (10.8). This interpretation is supported by another experiment in which we compared tryptophan and proline. We found that gas-phase reverse micelles show less discrimination between tryptophan (pI 5.9) and proline (pI 6.3) than between tryptophan and arginine. Again, we note that pI values of these amino acids are adopted from their aqueous solutions, and are used here only as a guide to predict amino acid responsiveness in the gas phase and in micellar environments.

This interpretation does not completely explain the selective encapsulation of different amino acids by reverse micelles. For example, the methanol–water solution of NaAOT (1.0×10^{-3} M), arginine (0.1×10^{-3} M) and tryptophan (0.1×10^{-3} M) has a similar pH (7.5) to that of NaAOT (1.0×10^{-3} M) and tryptophan (0.2×10^{-3} M) (pH 7.9). Considering the latter solution was used for obtaining neutral tryptophan-encapsulating reverse micellar ions in Fig. 2b, we would have expected some neutral tryptophan-entrapped reverse micellar ions from the NaAOT/arginine + tryptophan solution as well. However, no significant amount of tryptophan was detected in Fig. 6. Two possible reasons could be proposed. First, the spraying droplets may have a greater fraction of protonated arginine than that of neutral tryptophan, resulting in most reverse micelles being occupied by protonated arginine instead of neutral tryptophan. Second, protonated arginine establishes strong electrostatic interactions with AOT polar heads at the interface, which pulls the AOT head groups together and increases the curvature and rigidity of the micelle interface, leading to expulsion of neutral tryptophan from the curved surfactant-head region (*i.e.* a squeezing-out effect[28,30]). The strong electrostatic interactions also inhibit change in micellar shape, a change which is required to accommodate neutral tryptophan at the curved interfacial region.[37] Consequently, protonated arginine acts as a stripping agent and neutral tryptophan molecules can no longer be incorporated in its presence. A similar phenomenon occurred in the presence of protonated tryptophan and neutral aspartic acid. This indicates that electrostatic associations between AOT anionic polar heads and positively charged amino acids are more important than other factors for controlling amino acid solubilization in gas-phase reverse micelles. Note that selective extraction of different amino acids has been reported for NaAOT reverse micelles in supercritical fluids[5] and in isooctane,[68] but none of those experiments showed exclusive extraction with a high selectivity as presented in our gas-phase system.

IV. Conclusions

We have elucidated mechanisms involved in encapsulation of various hydrophilic and hydrophobic amino acids in gas-phase NaAOT reverse micelles. The experiment was designed for evaluations of the electrostatic and hydrophobic effects on the solubilization of amino acids. Hydrophilic amino acids are taken up inside micellar cavities *via* electrostatic interactions. Neutral tryptophan, on the other hand, intercalates in the interfacial region and acts as a co-surfactant. These phenomena could be expected from the hydrophobicities of

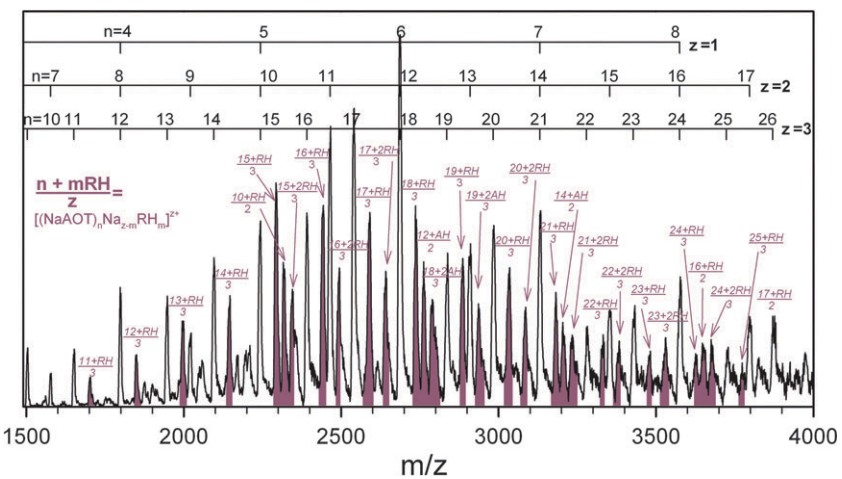

Fig. 6 ESI mass spectrum of an ESI solution containing NaAOT (1.0×10^{-3} M), arginine (0.1×10^{-3} M), and tryptophan (0.1×10^{-3} M) in methanol–water (1 : 1 volume ratio). Only protonated arginine (*RH*) was encapsulated into gas-phase reverse micelles. No tryptophan was detected.

amino acids as determined from their partitioning between a hydrophobic environment and aqueous solution.[39–41] Solubilization of hydrophobic tryptophan requires forces contributed from both the hydrophobic effect of amino acid side chain and the electrostatic interactions between amino acid backbone $-H_3N^+-C^{\alpha}-COO^-$ and NaAOT. Protonation of tryptophan could significantly improve its incorporation efficiency in gas-phase reverse micelles, and displaces its site locations from the interfacial region to the micellar core. In contrast, protonation of glycine has little effect on its encapsulation in gas-phase reverse micelles. Encapsulation of protonated amino acids makes the micellar structure more rigid and stable,[37] and inhibits further incorporation of neutral amino acids at the interfacial region. This explains the experimental observations that gas-phase reverse micelles show preferential encapsulation of tryptophan over aspartic acid, and of arginine over tryptophan, consistent with the order of their isoelectric points (*i.e.* protonation capabilities) in aqueous solutions.

The present study shows that electrostatic interactions are much stronger than the hydrophobic effect for driving solubilization of amino acids in gas-phase reverse micelles. It demonstrates that gas-phase reverse micelles are able to act as nanometre-sized vehicles for *selective* transport of hydrophilic and hydrophobic amino acids into the gas phase. This may lead to potential applications of reverse micelles in gas-phase separation and mass analysis of neutral and charged amino acids. It also provides insight on the dynamics of amino acid transport in atmospheric reverse micelle aerosols.

Acknowledgements

This work was supported by the Donors of the American Chemical Society Petroleum Research Fund (PRF #48208-G6), CUNY Collaborative Grant, Queens College Research Enhancement Funds, and PSC-CUNY Research Awards. J.L. also acknowledges support by the National Science Foundation CAREER Award (Grant No. CHE-0954507). Y.F. is the recipient of the CUNY Doctoral Student Research Grant and Research Excellence Award in 2010. A.B. acknowledges support by Queens College Undergraduate/Mentoring Education Initiative.

References

1 P. L. Luisi, M. Giomini, M. P. Pileni and B. H. Robinson, *Biochim. Biophys. Acta*, 1988, **947**, 209–246.
2 K. Kon-no, *Surface and Colloid Science*, 1993, **15**, 125–151.
3 M. P. Pileni, *Studies in Physical and Theoretical Chemistry 65: Structure and Reactivity in Reverse Micelles*, Elsevier Science Publishers, Amsterdam, 1989.
4 R. W. Gale, J. L. Fulton and R. D. Smith, *J. Am. Chem. Soc.*, 1987, **109**, 920–921.
5 R. M. Lemert, R. A. Fuller and K. P. Johnston, *J. Phys. Chem.*, 1990, **94**, 6021–6028.
6 A. M. Middlebrook, D. M. Murphy and D. S. Thomson, *J. Geophys. Res.*, 1998, **103**, 16475–16483.
7 H. Tervahattu, K. Hartonen, V.-M. Kerminen, K. Kupiainen, P. Aarnio, T. Koskentalo, A. F. Tuck and V. Vaida, *J. Geophys. Res.*, 2002, **107**, 4053.
8 H. Tervahattu, J. Juhanoja and K. Kupiainen, *J. Geophys. Res.*, 2002, **107**, 4319.
9 D. M. Murphy, D. S. Thomson and M. J. Mahoney, *Science*, 1998, **282**, 1664–1669.
10 J. P. Reid and R. M. Sayer, *Sci. Prog.*, 2002, **85**, 263–296.
11 P. S. Gill, T. E. Graedel and C. J. Weschler, *Rev. Geophys.*, 1983, **21**, 903–920.
12 G. B. Ellison, A. F. Tuck and V. Vaida, *J. Geophys. Res.*, 1999, **104**, 11633–11643.
13 C. M. Dobson, G. B. Ellison, A. F. Tuck and V. Vaida, *Proc. Natl. Acad. Sci. U. S. A.*, 2000, **97**, 11864–11868.
14 D. J. Donaldson, A. F. Tuck and V. Vaida, *Phys. Chem. Chem. Phys.*, 2001, **3**, 5270–5273.
15 K. A. Mace, R. A. Duce and N. W. Tindale, *J. Geophys. Res.*, 2003, **108**, 4338.
16 B. T. Mader, J. Z. Yu, J. H. Xu, Q. F. Li, W. S. Hu, R. C. Flagan and J. H. Seinfeld, *J. Geophys. Res.*, 2004, **109**, D06206.
17 K. Matsumoto and M. Uematsu, *Atmos. Environ.*, 2005, **39**, 2163–2170.
18 J. Zahardis, S. Geddes and G. A. Petrucci, *Int. J. Environ. Anal. Chem.*, 2008, **88**, 177–184.
19 N. P. Barrera, N. D. Bartolo, P. J. Booth and C. V. Robinson1, *Science*, 2008, **321**, 243–246.
20 R. Neutze, R. Wouts, D. v. d. Spoe, E. Weckert and J. Hajdu, *Nature*, 2000, **406**, 752–757.
21 M. Yamashita and J. B. Fenn, *J. Phys. Chem.*, 1984, **88**, 4451–4459.
22 J. B. Fenn, M. Mann, C. K. Meng, S. F. Wong and C. M. Whitehouse, *Science*, 1989, **246**, 64–71.
23 Y. Fang, A. Bennett and J. Liu, *Int. J. Mass Spectrom.*, 2010, **293**, 12–22.
24 M. Wong, J. K. Thomas and T. Nowak, *J. Am. Chem. Soc.*, 1977, **99**, 4730–4736.
25 H.-S. Tan, I. R. Piletic and M. D. Fayer, *J. Chem. Phys.*, 2005, **122**, 174501.
26 M. R. Harpham, B. M. Ladanyi and N. E. Levinger, *J. Phys. Chem. B*, 2005, **109**, 16891–16900.
27 P. A. Pieniazek, Y.-S. Lin, J. Chowdhary, B. M. Ladanyi and J. L. Skinner, *J. Phys. Chem. B*, 2009, **113**, 15017–15028.
28 E. B. Leodidis and T. A. Hatton, *J. Phys. Chem.*, 1990, **94**, 6400–6411.
29 E. B. Leodidis and T. A. Hatton, *J. Phys. Chem.*, 1990, **94**, 6411–6420.
30 E. B. Leodidis, A. S. Bommarius and T. A. Hatton, *J. Phys. Chem.*, 1991, **95**, 5943–5956.
31 E. B. Leodidis and T. A. Hatton, *J. Phys. Chem.*, 1991, **95**, 5957–5965.
32 E. B. Leodidis and T. A. Hatton, *J. Colloid Interface Sci.*, 1991, **147**, 163–177.
33 M. Adachi, M. Harada, A. Shioi and Y. Sato, *J. Phys. Chem.*, 1991, **95**, 7925–7931.
34 M. M. Cardoso, M. J. Barradas, M. T. Carrondo, K. H. Kroner and J. G. Crespo, *Bioseparation*, 1998, **7**, 65–78.
35 M. M. Cardoso, M. J. Barradas, K. H. Kroner and J. G. Crespo, *J. Chem. Technol. Biotechnol.*, 1999, **74**, 801–811.
36 X. Fu, J. Li, Y. Ma, L. Zhang, D. Wang and Z. Hu, *Colloids Surf., A*, 2001, **179**, 1–10.
37 R. Rinaldi, P. L. O. Volpe and I. L. Torriani, *J. Colloid Interface Sci.*, 2008, **318**, 59–67.
38 P. Vollhardt and N. Schore, *Organic Chemistry*, W. H. Freeman and Company, New York, 2009.
39 Y. Nozaki and C. Tanford, *J. Bio. Chem.*, 1971, **246**, 2211–2217.
40 W. C. Wimley, T. P. Creamer and S. H. White, *Biochemistry*, 1996, **35**, 5109–5124.
41 W. C. Wimley and S. H. White, *Nat. Struct. Biol.*, 1996, **3**, 842–848.
42 R. Allen, S. Bandyopadhyay and M. L. Klein, *Langmuir*, 2000, **16**, 10547–10552.
43 A. I. Bulavchenko, A. F. Batishchev, E. K. Batishcheva and V. G. Torgov, *J. Phys. Chem. B*, 2002, **106**, 6381–6389.
44 Y. Fang and J. Liu, *J. Phys. Chem. A*, 2009, **113**, 11250–11261.
45 D. Gerlich, in *State-Selected and State-to-State Ion-Molecule Reaction Dynamics. Part I. Experiment*, ed. C. Y. Ng and M. Baer, John Wiley & Sons, Inc., New York, 1992, vol. 82, pp. 1–176.
46 M. Sharon, L. L. Ilag and C. V. Robinson, *J. Am. Chem. Soc.*, 2007, **129**, 8740–8746.
47 D. Bongiorno, L. Ceraulo, A. Ruggirello, V. T. Liveri, E. Basso, R. Seraglia and P. Traldi, *J. Mass Spectrom.*, 2005, **40**, 1618–1625.

48 G. Giorgi, L. Ceraulo and V. T. Liveri, *J. Phys. Chem. B*, 2008, **112**, 1376–1382.
49 G. Giorgi, E. Giocaliere, L. Ceraulo, A. Ruggirello and V. T. Liveri, *Rapid Commun. Mass Spectrom.*, 2009, **23**, 2206–2212.
50 K. Mukherjee, S. P. Moulik and D. C. Mukherjee, *Langmuir*, 1993, **9**, 1727–1730.
51 J. F. D. L. Mora, *J. Fluid Mech.*, 1992, **243**, 561–574.
52 J. S. Klassen, Y. Ho, A. T. Blades and P. Kebarle, *Adv. Gas-Phase Ion Chem.*, 1998, **3**, 255–318.
53 P. Kebarle, *J. Mass Spectrom.*, 2000, **35**, 804–817.
54 S. E. Rodriguez-Cruz, J. T. Khoury and J. H. Parks, *J. Am. Soc. Mass Spectrom.*, 2001, **12**, 716–725.
55 S. K. Chowdhury, V. Katta and B. T. Chait, *Rapid Commun. Mass Spectrom.*, 1990, **4**, 81–87.
56 R. M. Moision and P. B. Armentrout, *J. Am. Soc. Mass Spectrom.*, 2007, **18**, 1124–1134.
57 A. N. Krutchinsky, I. V. Chernushevich, V. L. Spicer, W. Ens and K. G. Standing, *J. Am. Soc. Mass Spectrom.*, 1998, **9**, 569–579.
58 D. J. Douglas and J. B. French, *J. Am. Soc. Mass Spectrom.*, 1992, **3**, 398–408.
59 K. M. Ervin and P. B. Armentrout, *J. Chem. Phys.*, 1985, **83**, 166–189.
60 F. M. Menger and G. Saito, *J. Am. Chem. Soc.*, 1978, **100**, 4376–4379.
61 A. M. Maitra and P. K. Patanjali, in *Surfactants in Solution*, ed. K. L. Mittal and P. Bothorel, Plenum Press, New York, 1986, vol. 5, p. 581.
62 L. J. Magld, K. Kon-no and C. A. Martin, *J. Phys. Chem.*, 1981, **85**, 1434–1439.
63 E. Bardez, E. Monnier and B. Valeur, *J. Phys. Chem.*, 1985, **89**, 5031–5036.
64 R. M. Moision and P. B. Armentrout, *J. Phys. Chem. A*, 2002, **106**, 10350–10351-10362.
65 S. J. Ye, R. M. Moision and P. B. Armentrout, *Int. J. Mass Spectrom.*, 2005, **240**, 233–248.
66 M. J. Locke and R. T. McIver, Jr., *J. Am. Chem. Soc.*, 1983, **105**, 4226–4232.
67 J. Faeder and B. M. Ladanyi, *J. Phys. Chem.*, 2005, **109**, 6732–6740.
68 M. Hebrant and C. Tondre, *Anal. Sci.*, 1998, **14**, 109–115.

